An update on the GlueX II and Jefferson Lab η Factory experiments (as part of the Jeopardy exercise for PAC 48)

(Dated: June 5, 2020)

I. INTRODUCTION

The Hall D experimental facility at Jefferson Lab contains a unique energy-tagged, high-intensity real photon beam and a multipurpose large-acceptance spectrometer that was designed and constructed by the GlueX Collaboration. The initial data taking phase of the GlueX experiment was presented in 2006 to PAC 30 [1] and was approved for 100 days of beam with a focus on searching for hybrid mesons that have explicit gluonic degrees of freedom. While hadron spectroscopy was the physics driver for the GlueX detector, the collaboration realizes that beamline, detector, and at some level, the very same data sets used for hadron spectroscopy, provide opportunities to explore a variety of topics in a manner very similar to more traditional high-energy physics experiments. While some of these topics may be explored with existing data, others need specialized configurations, or augmentation of the baseline detector hardware, and they may seek approval from the PAC to motivate these dedicated runs or detector changes. In addition, the GlueX Collaboration has defined an internal process of *endorsement* for these distinct experimental offshoots. Endorsed proposals have the backing of the entire collaboration to staff shifts, calibrate and process data, and provide expertise to support the subsequent analysis of data. (The endorsement process was detailed in Ref. [2] and conveyed to the PAC and Jefferson Lab management.)

In this update we address three endorsed proposals that were previously approved by the PAC. Broadly speaking, two of these proposals seek to expand the initial GlueX physics program by providing increased sensitivity to states with $s\bar{s}$ quarks through higher intensity running and an upgrade to the particle identification system. This allows a complete study of the light quark conventional mesons and hybrid spectrum, including, in principle, measurements of the mixing between isoscalar $s\bar{s}$ and non-$s\bar{s}$ states, features that are calculable by lattice QCD [3]. The third proposal uses the high-intensity photon beam and an enhanced calorimeter for photon detection to conduct studies of η decays with unprecedented precision. Such studies will enable searches for light dark matter candidates, improved limits on charge conjugation and parity violating decays, as well as further our knowledge of chiral perturbation theory.

II. STATUS OF PROPOSALS AND BEAM TIME ALLOCATIONS

The initial allocation of beam time for the GlueX experiment came from a 2006 proposal (E12-06-102) to PAC 30 [1]. A total of 120 days were approved and there was a plan to use these days in three phases: detector commissioning, analysis commissioning, and production running at rate[1] of 10^7 γ/s. While this proposal was sufficient to make a number of new photoproduction measurements, it was insufficient to carry out the full GlueX hybrid meson search program in that it lacked adequate π/K separation to explore hybrids with hidden strangeness and the anticipated data set would be statistics limited in key hybrid search channels such as $\gamma p \to \eta' \pi p$. In 2012, before detector construction was completed, the collaboration presented a proposal (E12-12-002) to PAC 39 [4], which proposed collecting an order of magnitude more data over the initial GlueX run and developing a particle identification (PID) system. This proposal was conditionally approved pending design of the PID detector. Since some aspects of the program only need more statistics and not necessarily augmented PID, the collaboration submitted a proposal (E12-13-003) to PAC 40 to cover running GlueX at high intensity without a PID detector [5]. That proposal was approved for 200 days. In the early part of 2014 the collaboration submitted a successful competitive proposal to reuse the priceless synthetic quartz radiator system from the decommissioned BaBar DIRC (Detection of Internally Reflected Cherenkov light) [6]. We resubmitted proposal C12-12-002 to PAC 42 in 2014 with a design for a GlueX DIRC based on these components [7]. This proposal was approved by PAC 42 for 200 days of production running plus 20 days to commission the new DIRC. The lab management elected to merge proposals E12-12-002 and E12-13-003 based on their overlapping objectives. From here on we refer to this program as "GlueX II" (to distinguish it from the original three-phase GlueX startup covered by E12-06-102). In some proposal documents one will find the notation "GlueX Phase IV," which we now treat as synonymous with "GlueX II." As of this writing the GlueX II program has commissioned the DIRC and completed 38 days of production running.

In parallel with the development of the GlueX II program is a complementary effort called the "Jefferson Lab Eta Factory" (JEF) to explore rare decays of the $\eta^{(\prime)}$ meson. The $\eta^{(\prime)}$ meson, with the quantum numbers of the vacuum, provides a unique, flavor-conserving laboratory to probe the isospin-violating sector of low-energy QCD and to search for new physics Beyond the Standard Model (BSM). The Hall D beamline, through photoproduction, will generate a sample of η and η' that is com-

[1] Throughout this document when we refer to beam photon rates we imply number of photons on target with an energy in the region of enhanced linear polarization, the "coherent peak," produced by the diamond radiator.

Table I. A summary of the three PAC proposals discussed in this update.

Topic	Proposal Number	Commissioning Approved	Commissioning Completed	Production Approved	Production Completed
GlueX II with DIRC	E12-12-002	20	14	200	38
GlueX II	E12-13-003	0	0	200	38
JEF	E12-12-002A	0	0	100	0
Total Unique	-	20	14	200	38

parable or exceeds the statistical precision of other facilities worldwide and has unique kinematics (large boost in the lab) that is advantageous for suppressing backgrounds. This program relies on an upgrade to GlueX forward calorimeter (FCAL) to enhance sensitivity to rare decays through improved resolution and reduced background. The upgrade, called FCAL 2 in this document, replaces the inner section of the FCAL lead-glass modules with smaller, higher-resolution, more radiation-hard lead tungstate modules. The JEF program was is detailed in a proposals to PAC 42 and 45 [8, 9], and the proposal E12-12-002A was approved by PAC 45 to run concurrently for 100 days with the GlueX II program described above. While the presence of the GlueX DIRC detector material slightly reduces photon detection efficiency and enhances background, the JEF physics goals can still be achieved through concurrent running. The calorimeter insert benefits the GlueX II spectroscopy program by providing reduced background through enhanced resolution and mitigates detector lifetime concerns due to radiation damage.

In summary there are a total of 220 unique PAC days approved for the GlueX II and JEF programs. At present the hardware upgrades for GlueX II have been commissioned and 38 days of production beam have been collected. Design and construction of the FCAL 2 is underway, and the detector must be commissioned before the JEF physics program can begin. We now review the status of these proposal since they were originally submitted to the PAC.

III. UPDATES TO THE GLUEX II PROGRAM

The motivation for the GlueX II proposal has only strengthened in the time since the original proposal was submitted. The desire to explore quark flavor content of the hybrid meson spectrum as well as conventional states through their decays to strange and non-strange mesons continues to be of interest. Recently, these techniques of using decay to infer quark content, which previously relied on assumption of the "OZI rule" have been validated by Lattice QCD calculations that can now measure couplings to strange and non-strange final states [10, 11]. Evidence of the existence of an exotic π_1 hybrid meson continues to accumulate: a recent coupled-channel analysis of $\eta\pi$ and $\eta'\pi$ pion-production data from the COMPASS experiment indicates exotic P-wave enhancements in both channels are consistent with the presence of a single hybrid resonance [12]. The GlueX II program is in a position to advance the field by providing data from polarized photoproduction, a complementary scheme in which information about production mechanism can be gleaned, as well as attempting to uncover additional states in the hybrid spectrum. In order to do this, one needs at least the statistical precision provided by the PAC-approved GlueX II data set.

A. Construction and operation of the DIRC

The physics goals of the GlueX II proposal relied on extending π/K separation at a level of at least 3σ up to 3.7 GeV/c, providing the purity needed to explore to $s\bar{s}$ hybrid decays to strange final states. The enhanced PID capability comes from utilizing a ring imaging Cherenkov detector that spans the forward acceptance ($\theta < 10°$) of the GlueX detector. The design of this detector makes use of one-third of the BaBar DIRC radiator system in the form of four "bar boxes." The final design is similar to that in the original proposal [7] with the exception that boxes are oriented horizontally and pairs of boxes (two above and below the beamline) are individually coupled to an optical readout system which were designed and constructed specifically for the GlueX DIRC. The three-year upgrade project had a budget of $1.8M and underwent an external technical design review organized by Jefferson Lab in fall of 2015.

The ability to reuse the BaBar radiators took advantage of a fabrication effort centered at SLAC that spanned many years at a cost of tens of millions of dollars. It also posed challenges as four of the 5-m long bar boxes, each full of a fragile assembly of glued synthetic quartz components, had to be transported across the country and then used without modification in the GlueX apparatus. A support structure was designed on to hold the bar boxes in the GlueX configuration and mate them to the newly-designed and fabricated optical cameras that image the Cherenkov rings emerging from the radiator bars. The first of four bar boxes was successfully transported to Jefferson Lab in fall of 2017 and the remaining three were transported in summer of 2018. At the start of the spring 2019 run all four bar boxes were installed and one of the two optical cameras was instrumented, as shown

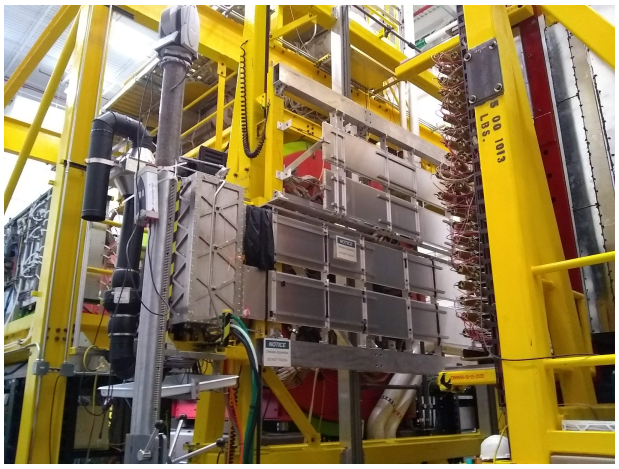

Figure 1. Four BaBar bar boxes transported to JLab and optical camera installed in the GlueX detector on the DIRC support structure in Hall D.

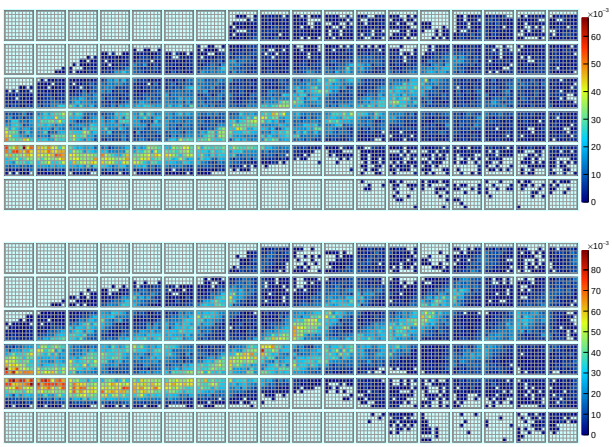

Figure 2. DIRC Cherenkov photon hit unnormalized hit occupancy over MAPMT plane for identified π^+ tracks, comparing data (top) with the expected distribution from GEANT MC simulation (bottom).

in Fig. 1. The full detector was installed and operational for commissioning by the fall of 2019. The optical cameras consist of multiple flat mirrors, immersed in water, that reflect the Cherenkov photons through a fused silica window to a plane of Multi-Anode PMTs (MAPMTs). Figure 2 shows a characteristic detected photon occupancy for identified pion tracks on the MAPMT plane, demonstrating the expected folded "ring" image, which compares well GEANT4 simulations.

The key performance metric for a ring imaging Cherenkov detector is the resolution on the angle of emitted Cherenkov photons for a single track $\sigma_\theta^{\text{track}}$. For a single charged particle produces, tens of Cherenkov photons are detected, each of which give a measure of the Cherenkov angle. Therefore, one can write the single track resolution as a sum of two components:

$$\left(\sigma_\theta^{\text{track}}\right)^2 = \left(\frac{\sigma_\theta^{\text{photon}}}{N_{\text{photons}}}\right)^2 + \left(\sigma^{\text{correlated}}\right)^2. \qquad (1)$$

In this expression the first term on the right hand side is the contribution to the resolution from each independent photon and the second term concerns resolution of quantities that are common to all photons emitted by a single track, *e.g.*, the incident angle of the track on the radiator. The resolution is a function of the three terms to the RHS and to understand detector performance and how to improve it, each terms should be individually considered. For example, global tracking resolution typically only affects $\sigma^{\text{correlated}}$, while optical quality of the system affects N_{photon} and $\sigma_\theta^{\text{photon}}$. The key performance property for the GlueX DIRC outlined in the design report was to achieve $\sigma_\theta^{\text{track}} = 2.5$ mrad, which would permit 3σ separation of pions and kaons at 3.7 GeV/c.

During the winter 2020 run commissioning data was collected with the GlueX DIRC fully instrumented. One feature of this data was that a small high-resolution tracking device was inserted at three different locations immediately upstream of the DIRC plane. This device allowed us to check and refine our ability to extrapolate tracks from the central GlueX tracking chambers to the downstream DIRC. Position and angle resolutions consistent with design assumptions were demonstrated. The commissioning data also provided opportunity to quantify photon yield and single photon resolution ($\sigma_\theta^{\text{photon}}$). These studies often rely on relatively pure samples of pions and kaons obtained from $\rho \to \pi^+\pi^-$ or $\phi \to K^+K^-$. Based on experience from SLAC [13] we anticipated a single photon resolution of about 10 mrad. The current GlueX single photon resolution exhibits position and reflection dependent features but is on average in the range of 7-8 mrad, as shown in Fig. 3, in agreement with GEANT4 simulations. The average number of detected photons per track observed in the GlueX data ranges from 15 to 35, depending on the track incident angle, which is consistent with the observed photon yield at BaBar. However, this photon yield is currently lower

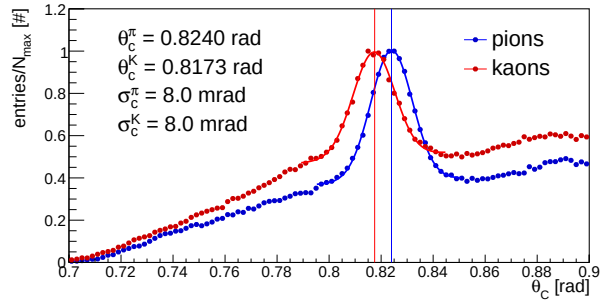

Figure 3. Cherenkov angle θ_C distribution for identified pions (blue) and kaons (red) with $p > 3.8$ GeV/c identified through the ρ and ϕ meson decays.

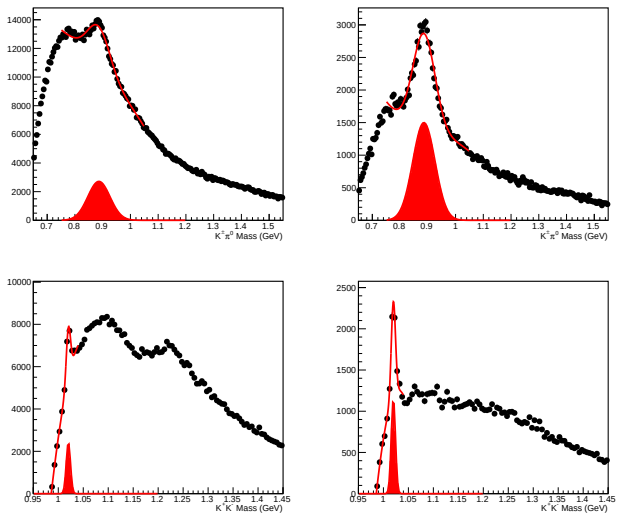

Figure 4. Mass distributions for $K^{\pm}\pi^0$ (top) and K^+K^- (bottom) from the reaction $\gamma p \to K^+K^-\pi^0 p$: (left) without utilizing the DIRC and (right) with a preliminary DIRC kaon identification applied.

than the expectation from GEANT4 simulations, in some extreme cases up to 50% less in regions of phase space. Similar discrepancies were noted by our colleagues who worked on the BaBar design, and in fact in some cases we see degradation with same individual quartz bars observed in BaBar. At present, we have met the 2.5 mrad design goal in some regions of phase space, but there is work left to do in fully understanding the photon yield and other aspects of reconstruction, like optical alignment, that will affect the resolution.

A small portion ($< 5\%$) of the 2020 dataset has been reconstructed for monitoring detector performance (see Sec. III B) where the preliminary DIRC performance can be demonstrated. Figure 4 shows the mass distribution of candidate $K^{\pm}\pi^0$ and K^+K^- pairs in the the reaction $\gamma p \to K^+K^-\pi^0 p$, with and without the using the DIRC to separate kaons from the significant pion background. In this reaction we expect significant contributions in the resonance decays of $K^* \to K^{\pm}\pi^0$ and $\phi \to K^+K^-$, which are clearly observed. The right panels show that the background beneath these resonances is significantly reduced when a preliminary DIRC kaon identification selection is applied. Many commissioning studies, such as this, are statistics limited by the small monitoring data set and will benefit tremendously from the reconstruction of the full spring 2020 GlueX II data set.

B. Readiness for data analysis

The GlueX II analysis program builds on the infrastructure developed to process and analyze the data acquired in the context of the original GlueX proposal. The scheme requires a well organized framework of software tools and people who are experts in monitoring and calibrating the individual detector components. At the completion of each data taking campaign the collaboration begins the calibration phase where specialized skims of data are used to perform calibration tasks on each detector. The results of these calibrations and the quality of the overall event reconstruction is then assessed through a series of successive "monitoring launches" where about 5% of the events in each run are reconstructed and hundreds of diagnostic plots are examined (*e.g.* see Fig. 4).

Once the software stack and calibrations are certified, the core reconstruction is performed using the resources of National Energy Research Scientific Computing Center (NERSC), a technique of pioneered by GlueX for event reconstruction at Jefferson Lab to alleviate load on the local computing farm. Reconstruction of the initial GlueX II data collected in January 2020 will be deployed at NERSC in June 2020, which, despite challenges with bringing the DIRC into the analysis flow, is the fastest we have started reconstruction after data acquisition.

The subsequent data analysis phase is also a product of years of development and refinement. It is not practical for any one analyst to stage and read the hundreds of terabytes of reconstructed data in order to search for the signal for a particular reaction. Instead the GlueX collaboration uses a system of "analysis launches" where the data are processed and tens of different reactions are simultaneously filtered from the data using standard selection criteria and a standard output. This output can then be used by individual analysts. A companion to these analyses is the ability to simulate the response of the detector. The collaboration has developed a detailed simulation based on the GEANT4 framework that incorporates the DIRC as well as other detector elements. The simulation is tuned to match to the time dependent features of the data, *e.g.*, even including noise from out-of-time events acquired during the actual run that is being simulated. The simulation can be deployed on a large scale using the Open Science Grid, and a web-based user interface has been developed to provide easy access to simulated data and ensure complex task of synchronizing software is performed correctly. The analysis and understanding of its performance has taken years to develop, was critical in publication of recent results from GlueX [14–17], and will be essential in the search for hybrid mesons using GlueX I and GlueX II data.

IV. UPDATES TO THE JEF PROGRAM

Though the JEF experiment will offer sensitive probes for a broad range of physics topics as described in [8, 9], its primary objectives are: (1) A search for new sub-GeV gauge bosons; (2) direct constraints on new C-violating, P-conserving reactions (CVPC); (3) tests of low-energy QCD via precision measurements; and (4) an accurate determination of the quark mass ratio, $\mathcal{Q} =$

$(m_s^2-\hat{m}^2)/(m_d^2-m_u^2)$ with $\hat{m}=(m_u+m_d)/2$, via $\eta \to 3\pi$.

About 85% of matter in the universe is Dark Matter (DM) whose constituents and interactions are unknown other than its gravitational properties. The stability of Dark Matter (DM) suggests that there may be a dark sector consisting of a rich symmetry structure with new forces and new particles. The dark sector may include one or more mediator particles coupled to the SM via portals. The gauge and Lorentz symmetries of the Standard Model (SM) greatly restrict the ways in which the mediator can couple to the SM. The most important portals are [18]: the vector, scalar, pseudoscalar and fermion. Over the past decades, intensive efforts at the Large Hadron Collider (LHC) and underground laboratories have born no fruit for Weakly Interacting Massive Particles (WIMP), the simplest possible model for dark matter.

There is a strong consensus among the physics community about the vital importance of broadening the scope of searches [18–20], both in the parameter space and in experimental approaches. The top-down models predict light mediators below GeV scale [21, 22]. These light states would have escaped detection thus far if they are very weakly coupled to the Standard Model. Recently, sub-GeV mediators have gained strong motivation, driven partly by several observed anomalies. The reported excesses in high-energy cosmic rays could be explained by dark matter annihilation [23, 24]. The muon $g-2$ anomaly [25–27] and an anomalous e^+e^- resonance observed in ^{8}Be decay [28, 29] can be resolved by new gauge bosons. In addition, scalar- or vector-mediated dark forces can also explain long-standing issues with galactic rotation curves and can solve small scale structure anomalies in dwarf galaxies and subhalos, while satisfying constraints on larger galaxy and cluster scales [30–32]. If these phenomena are interpreted in terms of new physics, all point toward mediator particles in the MeV–GeV mass range. Figure 5 shows a map of the parameter landscape for the global efforts on the BSM searches. LHC can realistically pick up new physics in the upper-right corner of the map for the coupling constant of $\alpha_X \sim \alpha_{SM}$ and the mass scale of $m_X \sim 1$ TeV, and the Lepton Flavor Violation (LFV) and sub-atomic Electric Dipole Moment (EDM) searches can explore the bottom region for $\alpha_X \leq 10^{-6}$ and a broad range of m_X up to 1000 TeV.

Compared to the original JEF proposals [8, 9] submitted to the previous PACs, the scope of the JEF physics has been expanded mainly in two areas: (1) new physics searches have been broadened by not only searching for a leptophobic dark vector boson (B') [33] but also including dark photon [26, 34–36], hadrophilic scalar [37], and Axion-Like Particles [38–40], probing three out of four the most motivated portals coupling the SM sector to the dark sector; (2) production of η' simultaneously with η at the similar rate will extend the mass coverage of new mediator search to ~ 1 GeV. These new sub-GeV gauge bosons will be probed in the following processes.

Vector: a leptophobic vector boson (B') [33] coupling to baryon number can be searched for via

$$\eta, \eta' \to B'\gamma \to \pi^0\gamma\gamma \quad (0.14 < m_{B'} < 0.62 \text{ GeV});$$
$$\eta' \to B'\gamma \to \pi^+\pi^-\pi^0\gamma \quad (0.62 < m_{B'} < 1 \text{ GeV}).$$

A dark photon (or leptophilic vector boson) kinetically mixing to the Standard model photon [26, 34–36] can be searched for using

$$\eta, \eta' \to A'\gamma \to e^+e^-\gamma.$$

Scalar: a hadrophilic [27, 37] scalar scan be searched for using

$$\eta \to \pi^0 S \to \pi^0\gamma\gamma,\ \pi^0 e^+e^- \quad (10 \text{ MeV} < m_S < 2m_\pi);$$
$$\eta, \eta' \to \pi^0 S \to 3\pi,\ \eta' \to \eta S \to \eta\pi\pi \quad (m_S > 2m_\pi).$$

Axion-Like Particle: light pseudoscalars [41–44] can be searched for via

$$\eta, \eta' \to \pi\pi a \to \pi\pi\gamma\gamma,\ \pi\pi e^+e^-.$$

The JEF program will focus on the sub-GeV mediators for interactions that can be even "stronger than weak" as shown in Fig. 5. Even though LFV and EDM may stretch to the small mass range and overlap some of territory within JEF's interest, however, LFV requires flavor-changing and EDM is sensitive to CP-violating physics. Therefore, η/η' decays used in the JEF experiment offer a unique niche for new physics that are flavor-conserving, light quark-coupling, and CP-conserving. Figure 6 gives an example for the sensitivity of the JEF experiment. With 100 day's beam time, a study of $\eta \to \gamma + B'(\to \gamma + \pi^0)$ will improve the existing bounds by two orders of magnitude, with sensitivity to the baryonic fine structure constant α_B as small as 10^{-7}, indirectly constraining the existence of anomaly cancelling fermions at the TeV-scale.

A. Design of the FCAL upgrade

The JEF experiment requires an upgrade of the inner part of the GlueX lead glass forward calorimeter with high-granularity, high-resolution $PbWO_4$ crystals. The calorimeter will improve the separation of clusters in the forward direction and the energy resolution of reconstructed photons by about a factor of two. The size of the lead tungstate insert is 1 m×1 m. The insert is an array of 50×50 crystal modules with a beam hole of 2×2 modules in the middle and consists of 2496 modules. Each crystal has the following dimension: 2 cm×2 cm×20 cm. Crystals are purchased from two vendors: SICCAS (China) and CRYTUR (Czech republic). CRYTUR crystals are know to have slightly better radiation properties and will be used for the instrumentation of three inner layers of the calorimeter insert. Properties of recently produced crystals have been studied in detail and can be found in Ref. [46]. SICCAS crystals with the length of 18 cm

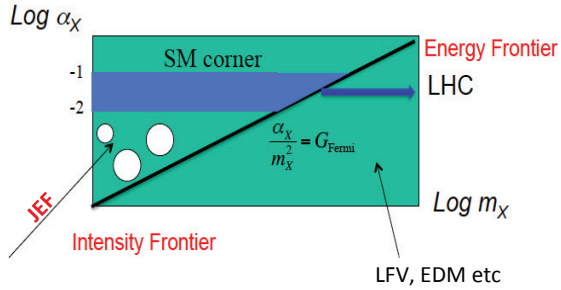

Figure 5. A sketch of the parameter landscape for BSM physics searches: the coupling constant α_X vs. the mass m_X [45].

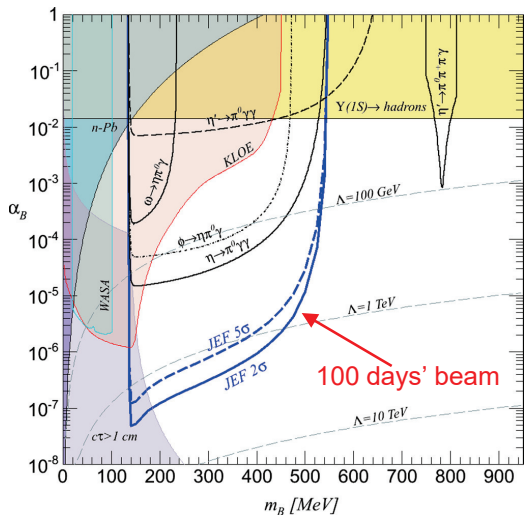

Figure 6. Current exclusion regions for a leptophobic gauge boson B' [33], with the proposed search region via $\eta \to \gamma + B'(\to \gamma + \pi^0)$ labelled "JEF" for the coupling vs. mass plane. Dashed gray contours denote the upper bound on the mass scale Λ for new electroweak fermions needed for anomaly cancellation.

were used in the hybrid calorimeter (HyCal) in the experimental Hall B [47]. Crystals from these vendors were also chosen for the instrumentation of the Neutral Particle Spectrometer, which is being currently constructed in Hall C.

The size of the FCAL 2 insert may slightly vary depending on availability of funds. The project is funded by the Jefferson Lab. We also applied for the NSF grand (PI is Prof. L. Gan from the University of North Carolina in Wilmington and co-PI is Prof. C. Meyer from Carnegie Mellon University). In the next section, we will describe the design of $PbWO_4$ modules and the status of the project.

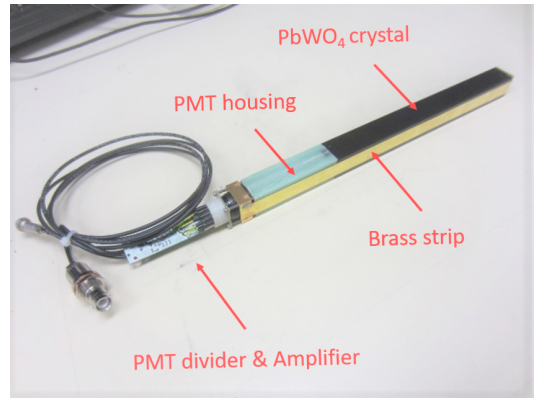

Figure 7. $PbWO_4$ module used in the FCAL 2 calorimeter prototype.

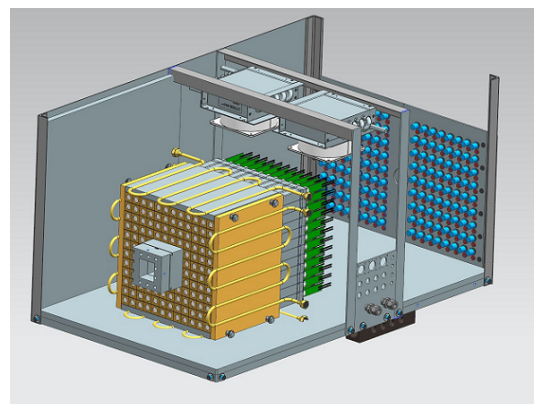

Figure 8. Schematic view of the Compton calorimeter used in the Hall D PrimEx experiment.

1. *Module design*

Design of the $PbWO_4$ module is based on the HyCal calorimeter, which was used in three experiments in Hall B (PrimEx-I, PrimEx-II and PRad). Schematic view of the module is presented in Fig. 7. The lead tungstate crystal is wrapped with the reflective material (ESR) and Tedlar. The crystal is attached to the PMT housing. Two flanges are positioned at the crystal and housing ends and are connected together using brass strips, which are brazed to the flanges. Four screws on the PMT housing flange provide strip tension and hold the assembly together. A Hamamatsu PMT 4125 is inserted inside the housing and is coupled to the crystal using an optical grease. The PMT is pushed towards the crystal by using a G10 plate and four screws. The PMT is read out using an active base, which was designed for the Hall C lead tungstate calorimeter (NPS) [48]. The base combines a voltage divider and an amplifier powered by the current flowing through the divider.

In Summer 2018 we constructed a small calorimeter

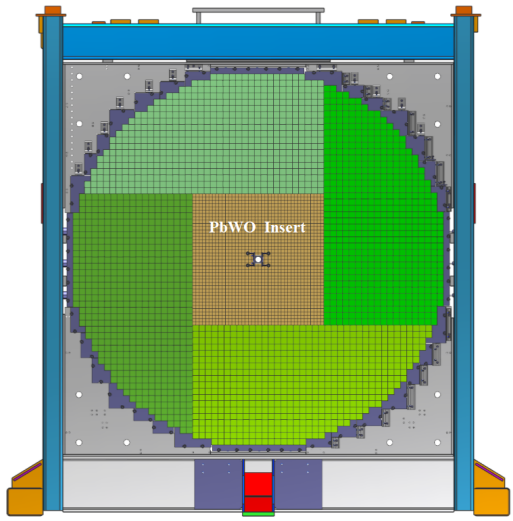

Figure 9. FCAL 2 frame with calorimeter modules installed: $PbWO_4$ crystals (brown area), lead glass blocks (green).

prototype consisting of 12×12 modules. The prototype layout is presented in Fig. 8. The calorimeter was successfully operated during the PrimEx-η experiment (E12-10-011) in Spring 2019 and used for the reconstruction of Compton events. The calorimeter was also tested during several GlueX high-luminosity runs.

Some modifications have been recently made in the module design: (1) We performed a detailed study of the PMT magnetic field shielding using magnetic fields produced by Helmholtz coils [49]. The shielding was also simulated using TOSCA field simulation program [50]. It was demonstrated, that the PMT housing made of the 1020 steel and two layers of mu-metal foils inside it will reduce the fringe filed of the Solenoid magnet (of about 50 Gauss) to the level sufficient for the reliable PMT operation (2) The magnetic field shielding requires to use a 3.5 cm long optical light guide between the crystal and PMT. Light collection was measured for different diameters of light guides and different coupling materials between the crystal and light guide using a test setup positioned downstream of the GlueX Pair Spectrometer [51] (3) Integrated to the GlueX detector, the Compton calorimeter allowed us to measure realistic operational conditions (PMT rates and anode current) for the FCAL 2 insert. These measurements were used to tune the design of the PMT active base.

The mechanical design of the $PbWO_4$ module has been finalized. Some details can be found on the FCAL 2 construction page [52]. We have already assembled a few modules and are ready for mass production.

2. *Calorimeter frame*

The crystal detector modules will be stacked in a 50×50 square array to be installed in the central region of the current FCAL as shown in Fig. 9. The light yield of the $PbWO_4$ crystal is highly temperature dependent ($\sim$ 2%/°C). In order to keep the detector array at a stable temperature, the frame for the upgraded FCAL 2 will be not only light-tight but also temperature stable, controlled by a cooling system. It will be fully funded and constructed by JLab. The engineering group in Hall D has been working on its development. The preliminary design is to have structured geometries in four corners of the frame (shown in Fig. 9) that match the shape of the detector assembly's outer edge. In each row, there will be aluminum cooling plates and shims in between the frame and the counter array. Those cooling plates will mechanically push against the detector assembly to provide alignment, to minimize the gaps between detector modules and to provide good thermal contact between the cooling plate and the calorimeter modules. The similar assembly scheme was used for the HyCal calorimeter and provided a temperature stability at the level of $\Delta T = \pm 0.1$°C. The detailed engineering drawings are currently in progress. The final review of the design and technical drawings will be completed by fall 2020.

V. SCHEDULING ISSUES AND OUTLOOK

Since all three proposals under discussion in this document are approved to run concurrently, there are some scheduling logistics that need to be examined. The key issue is whether the FCAL 2 upgrade can be installed and the JEF program can commence earlier enough such that there is sufficient time remaining in the ongoing GlueX II program for JEF to acquire at least 100 days of beam. We discuss first the status of procurement and construction of the FCAL 2 upgrade and then conclude with some comments about the overall schedule.

A. Status of the FCAL 2 construction project

The FCAL 2 construction project has a procurement and module fabrication phase that is expected to extend until Spring 2023. The installation phase of the project will then require at minimum six months of down time in Hall D.

1. *Procurement of components for the $PbWO_4$ insert*

We have already purchased and checked 64 crystals from CRYTUR, which are needed for the instrumentation of three inner layers of the calorimeter insert. Procurement of SICCAS crystals is organized in several steps. A total of 500 crystals were ordered in 2019. We

have already received the first batch of 132 crystals. Delivery of rest crystals is scheduled by the end of summer of 2020. Preparation of a new contract to order additional 500 more crystals is in progress. These crystals are expected to be delivered to the lab by the end of Spring 2021. The production rate of crystals by SICCAS is about 100 crystals a month. We plan to continue ordering crystals, depending on the availability of funds, and have all crystals ready by the end of Spring 2023.

Jefferson Lab has already purchased 500 PMTs from Hamamatsu, which is enough to start fabricating calorimeter modules. The lead time of PMTs is relatively short, 100 - 150 PMTs can be acquired a month. JLab has ordered read out and trigger electronics for about 1600 new calorimeter channels. This includes VXS crates (already delivered to the Lab), flash ADCs, crate readout controllers and trigger modules. Procurement of components needed for fabrication, such as light guides, soft iron PMT housings, mu-metal, flanges, etc. is in progress.

2. *Fabrication and installation schedule*

Fabrication of modules will be performed at Jefferson Lab in the special area in the TEDF building designated to the FCAL 2 project. All fabrication tools, procedures, and setups needed to perform QA checks of crystals are in place. We plan to assemble a few hundred modules by the end of this year. Based on our experience with the Compton Calorimeter, we can fabricate about ten modules per day, assuming two people working on it. At that pace the module fabrication will take 12-14 months, but can be done as crystals arrive.

Rebuilding the forward calorimeter can be done by a few groups of people performing different tasks in parallel. We expect that potentially the most time consuming procedure would be to refurbish the original lead glass modules of the FCAL after disassembling, since cleaning and rewrapping of the modules with an aluminized Mylar may be required. Preliminary schedules suggest that the full disassembly and reassembly of the calorimeter including all tasks such as cabling, testing, etc. will need at minimum six months of down time in Hall D. At present, it is anticipated that the earliest we would be ready for this installation task is during the summer of 2023.

B. Outlook

Both the GlueX II and JEF programs are focused on a variety of compelling topics that span the fields of nuclear and particle physics. The GlueX II program is underway, with the DIRC fully commissioned and about 20% of the approved beam time collected in early 2020. The JEF program has developed a mature design for the FCAL 2 upgrade, has begun procurement of crystals, and is ready to begin module fabrication.

The current climate adds a degree of uncertainty to any plan going forward. The GlueX II program may collect an additional 20 days of beam in 2020 assuming CEBAF resumes operations. In 2021 it is anticipated that the Hall D facility will collect data for other PAC-approved proposals. Some GlueX II running is likely in 2022 and 2023, which is around the time when FCAL 2 upgrade is projected to be ready for installation. It remains to be seen whether the available GlueX II beam time after the FCAL 2 upgrade will meet the requirements of the JEF program to reach its design potential. This will need to be revisited at a later date as the GlueX Collaboration continues to pursue a variety of the topics that one can address with the instrumentation in Hall D [2].

[1] The GlueX Collaboration, "Mapping the spectrum of light quark mesons and gluonic excitations with linearly polarized photons", a proposal to PAC 30, 2006, *https://www.jlab.org/exp_prog/proposals/06/PR12-06-102.pdf.*

[2] The GlueX Collaboration, "Future Physics in Hall D with the GlueX Detector," *GlueX-doc-3870-v11* (2019). *https://halldweb.jlab.org/DocDB/0038/003870/011/gluex_future.pdf.*

[3] J. J. Dudek *et al.* [Hadron Spectrum], Phys. Rev. D **88**, no.9, 094505 (2013) doi:10.1103/PhysRevD.88.094505 [arXiv:1309.2608 [hep-lat]].

[4] The GlueX Collaboration, "A study of meson and baryon decays to strange final states with GlueX in Hall D," a proposal to PAC 39, 2012, *https://www.jlab.org/exp_prog/proposals/12/PR12-12-002.pdf.*

[5] The GlueX Collaboration, "An initial study of mesons and baryons containing strage quarks with GlueX," a proposal to PAC 40, 2013, *https://www.jlab.org/exp_prog/proposals/13/PR12-13-003.pdf.*

[6] I. Adam *et al.* [BaBar DIRC], Nucl. Instrum. Meth. A **538**, 281-357 (2005) doi:10.1016/j.nima.2004.08.129

[7] The GlueX Collaboration, "A study of decays to strange final states with GlueX in Hall D using components of the BaBar DIRC," a proposal to PAC 42, 2014, *https://www.jlab.org/exp_prog/proposals/14/C12-12-002.pdf.*

[8] L. Gan et al., the updated JEF proposal to JLab PAC 45, 2017, *https://www.jlab.org/exp_prog/proposals/17/C12-14-004.pdf.*

[9] L. Gan et al., the JEF proposal to JLab PAC 42, 2014, *https://www.jlab.org/exp_prog/proposals/14/PR12-14-004.pdf.*

[10] J. J. Dudek *et al.* [Hadron Spectrum], Phys. Rev. D **93**, no.9, 094506 (2016) doi:10.1103/PhysRevD.93.094506 [arXiv:1602.05122 [hep-ph]].

[11] R. A. Briceno, J. J. Dudek, R. G. Edwards and

D. J. Wilson, Phys. Rev. D **97**, no.5, 054513 (2018) doi:10.1103/PhysRevD.97.054513 [arXiv:1708.06667 [hep-lat]].

[12] A. Rodas *et al.* [JPAC], Phys. Rev. Lett. **122**, no.4, 042002 (2019) doi:10.1103/PhysRevLett.122.042002 [arXiv:1810.04171 [hep-ph]].

[13] J. Va'vra *et al.*, Nucl. Instrum. Meth. A **718**, 541-545 (2013) doi:10.1016/j.nima.2012.11.112

[14] S. Adhikari *et al.* [GlueX], [arXiv:2003.08038 [nucl-ex]].

[15] S. Adhikari *et al.* [GlueX], Phys. Rev. C **100**, no.5, 052201 (2019) doi:10.1103/PhysRevC.100.052201 [arXiv:1908.05563 [nucl-ex]].

[16] A. Ali *et al.* [GlueX], Phys. Rev. Lett. **123**, no.7, 072001 (2019) doi:10.1103/PhysRevLett.123.072001 [arXiv:1905.10811 [nucl-ex]].

[17] H. Al Ghoul *et al.* [GlueX], Phys. Rev. C **95**, no.4, 042201 (2017) doi:10.1103/PhysRevC.95.042201 [arXiv:1701.08123 [nucl-ex]].

[18] J. Alexander *et al.*, arXiv:1608.08632 [hep-ph].

[19] R. Essig *et al.*, arXiv:1311.0029 [hep-ph].

[20] M. Battaglieri *et al.*, arXiv:1707.04591 [hep-ph].

[21] P. Fayet, Nucl. Phys. B **187**, 184 (1981).

[22] M. Goodsell, J. Jaeckel, J. Redondo and A. Ringwald, JHEP **0911**, 027 (2009) [arXiv:0909.0515 [hep-ph]].

[23] N. Arkani-Hamed, D. P. Finkbeiner, T. R. Slatyer and N. Weiner, Phys. Rev. D **79**, 015014 (2009) [arXiv:0810.0713 [hep-ph]].

[24] M. Pospelov and A. Ritz, Phys. Lett. B **671**, 391 (2009) [arXiv:0810.1502 [hep-ph]].

[25] M. Pospelov, Phys. Rev. D **80**, 095002 (2009) [arXiv:0811.1030 [hep-ph]].

[26] P. Fayet, Phys. Rev. D **75**, 115017 (2007) [hep-ph/0702176 [HEP-PH]].

[27] Y. S. Liu, I. C. Cloët and G. A. Miller, Nucl. Phys. B , 114638 (2019).

[28] A. J. Krasznahorkay *et al.*, Phys. Rev. Lett. **116**, 042501 (2016) [arXiv:1504.01527 [nucl-ex]].

[29] J. L. Feng, B. Fornal, I. Galon, S. Gardner, J. Smolinsky, T. M. P. Tait and P. Tanedo, Phys. Rev. Lett. **117**, 071803 (2016) [arXiv:1604.07411 [hep-ph]].

[30] S. Tulin and H. B. Yu, Phys. Rept. **730**, 1 (2018) [arXiv:1705.02358 [hep-ph]].

[31] S. Tulin, H. Yu, K.M. Zurek, Phys. Rev. Lett. 110, 111301 (2013).

[32] S. Tulin, H. Yu, K.M. Zurek, Phys. Rev. D 87, 115007-1 (2013).

[33] S. Tulin, Phys.Rev. D89, 114008 (2014).

[34] M. Reece and L. T. Wang, JHEP **0907**, 051 (2009) [arXiv:0904.1743 [hep-ph]].

[35] J. D. Bjorken, R. Essig, P. Schuster and N. Toro, Phys. Rev. D **80**, 075018 (2009) [arXiv:0906.0580 [hep-ph]].

[36] B. Batell, M. Pospelov and A. Ritz, Phys. Rev. D **79**, 115008 (2009) [arXiv:0903.0363 [hep-ph]].

[37] B. Batell, A. Freitas, A. Ismail and D. Mckeen, Phys. Rev. D **100**, 095020 (2019) [arXiv:1812.05103 [hep-ph]].

[38] M. Bauer, M. Neubert and A. Thamm, JHEP **1712**, 044 (2017) [arXiv:1708.00443 [hep-ph]].

[39] J. Hewett, *et al.* arXiv:1205.2671 [hep-ex].

[40] W. Altmannshofer, S. Gori and D. J. Robinson, Phys. Rev. D **101**, 075002 (2020) [arXiv:1909.00005 [hep-ph]].

[41] B. A. Dobrescu, G. L. Landsberg and K. T. Matchev, Phys. Rev. D **63**, 075003 (2001) [arXiv:hep-ph/0005308 [hep-ph]].

[42] D. Aloni, Y. Soreq and M. Williams, Phys. Rev. Lett. **123**, 031803 (2019) [arXiv:1811.03474 [hep-ph]].

[43] Y. Nomura and J. Thaler, Phys. Rev. D **79**, 075008 (2009) doi:10.1103/PhysRevD.79.075008 [arXiv:0810.5397 [hep-ph]].

[44] M. Freytsis and Z. Ligeti, Phys. Rev. D **83**, 115009 (2011) doi:10.1103/PhysRevD.83.115009 [arXiv:1012.5317 [hep-ph]].

[45] M. Pospelov, "Light Scalar and Vector Extensions of the Standard Model", Physics Seminars at JLab, May 16, 2014.

[46] T. Horn *et al.*, Nucl. Instrum. Meth. A **956** (2020).

[47] M. Kubantsev *et al.*, AIP Conference Proceedings (2006).

[48] V. Popov and H. Mkrtchyan *et al.*, Proceedings of the IEEE conference, California, 2012.

[49] A. Somov *et al.*, "Study of the FCAL 2 magnetic field shielding using Helmholz coils", GlueX-doc-4166, 2019.

[50] S. Glamazdin "Magnetic shielding simulation using TOSCA", `https://halldweb.jlab.org/talks/2018/Hybrid_FCal_shield.pdf`

[51] A. Somov, A. Asaturyan, J. Crafts, "Light collection studies of the $PbWO_4$ module with light guide", `https://halldweb.jlab.org/wiki/index.php/Light_Guide`.

[52] FCAL construction page `https://halldweb.jlab.org/wiki/index.php/FCAL_Insert`.